

Asismic and seismic slip on the Megathrust offshore southern Peru revealed by geodetic strain before and after the Mw8.0, 2007 Pisco Earthquake.

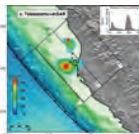
H. Perfettini¹, J.P. Avouac², H. Tavera³, A. Kasitsky², J.M. Nocquet⁴, F. Boudoux¹, M. Chlieh¹, A. Sladen², D. Farber¹, L. Audin¹, P. Soler¹
 1. IRD, France; 2. Caltech, USA; 3. IGP, Lima, Peru, France; 4. Geosciences Azur, France; 5. UCSC, USA

(1) Sismotectonic setting

The **Mañá Pisco earthquake** ruptured the subduction interface along which the Nazca plate subducts beneath the South American plate at about 6°N. Similar interplate $M > 8.0$ earthquakes have occurred offshore South and Central Peru in 1604, 1687, 1746, and 1868. In 2007, the same segment as the one that broke in 1746 ruptured again.

Distribution of recent large interplate earthquakes (light yellow ellipses). Approximate rupture areas for 1974, 1996, and 2007 (gray patches) from Langer and Spence (1995) and Frutiger et al. (2007). Ellipses for events without detailed models are scaled proportionally. The graph shows the distribution in time since 1604 of ruptures as a function of their along trench extent (adapted from Darbuth et al. 1990). NEIC Epicenter and GCMT centroid of the 2007 Pisco earthquake are indicated by the red star and an orange circle, respectively. Small black dots indicate aftershocks during the 49 days period following the mainshock recorded by a local network operated by IGP (stations: open triangles). From Sladen et al. (2009).

(2) The Mw8.0, 2007 Pisco Earthquake



In 2007 the rupture initiated north of Pisco and propagated towards the South producing up to 8 m of slip parallel to the Nazca-South America plate convergence. The source model shows that the earthquake broke two distinct asperities 60 seconds apart.

Surface projection of co-seismic slip distribution derived from the joint inversion of teleseismic waveforms and InSAR measurements of static ground motion. Slip contour lines every 1 m starting at 20 cm (gray areas where slip is larger, greater than 2 m are shown). Inset shows the estimated source time function. The red star marks the epicenter as located by USGS-NEIC. Bathymetry and topography are taken from the ETOPO2 and GTOPO30 datasets, respectively. From Sladen et al. (2009)

Abstract

We show that the Pisco earthquake ruptured two asperities within a patch that had remained predominantly locked in the interseismic period and triggered aseismic frictional relaxation on adjacent patches. The time evolution of afterslip, which is about 90% aseismic, is consistent with a rate-strengthening friction law. The most prominent afterslip patch reflects the influence of the Nazca Ridge. Aseismic sliding is also responsible for a locally low interseismic coupling in this area which seems to have acted as a systematic barrier to seismic rupture propagation respectively. Altogether, aseismic slip on the megathrust in the Peru Megathrust between latitude 11°S and 16°S is estimated to account for about 50-70 % of the slip budget. Aseismic slip on the megathrust in the study area (between latitudes 11°S and 16°S) is estimated to account for a large fraction of the slip budget. The megathrust appears to be paved with rate-strengthening and rate-weakening patches and the resulting pattern has a profound influence on its long term seismic behavior as well as on individual earthquakes.

(4) Geodetic Time Series

Time series of displacements recorded at the 6 GPS stations analyzed in this study. Error bars show 2- σ uncertainties.

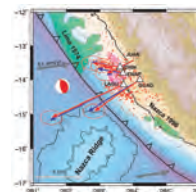
The continuous curve shows the theoretical displacements predicted from the best fitting afterslip model derived from the PCAEM (Kasitsky and Avouac, 2009) inversion of the time series for the time-evolution of four slip at depth.

(6) Interseismic coupling

The modeling of interseismic strain measured from GPS campaigns shows that on an average over the study area, aseismic slip in the interseismic period accounts for about 60% of interplate slip at depths greater than 40 km (the average interseismic coupling is 0.48). The Nazca ridge coincide with an area of locally low interseismic coupling.

Comparison of interseismic coupling with rupture areas of recent large earthquakes. Interseismic coupling, defined as $(1 - V_p/V_s)W$ where W is the interseismic slip rate and V_p the slip rate derived from the modeling of geodetic data collected between January 1993 and March 2001 all referenced to stable South America. The dots (white vectors) were corrected for 9 mm/yr of shortening across the Andes by least squares adjustment of the Euler pole describing the long term motion of the undeformed foreland with respect to South America. The small coupling along the trench may reflect lack of resolution there, except in the north where sea bottom measurements are available.

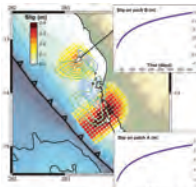
(3) Postseismic displacements



We installed a continuous GPS (GGPS) network of 5 GPS stations (Figure 1) which were in operation 33 days after the mainshock. The data analyzed here cover the time period until day 408 after the mainshock (see (4)). All horizontal displacements are transverse and reach up to 10cm over that period.

Co-seismic slip, aftershocks and postseismic displacements. Red vectors show horizontal postseismic displacements between days 20 and 408 after the mainshock and blue vectors show predictions from the best fitting afterslip model derived from the PCAEM inversion of the geodetic time series. The focal mechanism solution of the GCMT solution. The 2 m slip contour lines of the 2007 earthquake are shown in cyan (Sladen et al. 2009). Red dots show aftershock location from the IGP local seismic network. Green shading shows the rupture area of the Mw 8.1 1974 Lima, estimated from teleseismic waveforms and aftershocks (Langer and Spence, 1995), and of the Mw 7.1996 Nazca earthquake as derived from the joint inversion of InSAR and teleseismic waveforms (Frutiger et al. 2007).

(5) Afterslip Model



The post- and co-seismic slip distributions are observed to complement each other (the small overlap might simply reflect the smoothing effect of the regularization). This observation is consistent with the view that the shallow portion of the megathrust is paved with areas that are rate-weakening, while which earthquakes can nucleate and propagate, and areas that are rate-strengthening, within which slip is mostly aseismic. A most striking finding is that the prominent aseismic patch, labeled A, coincides with the northern side of the Nazca ridge where the 2007 rupture stopped.

We estimate that afterslip over the first 408 days released a geodetic moment of 3.3×10^{19} N.m (Mw = 6), representing nearly 28% of the coseismic moment released. Given that the cumulative moment released by all afterslip within the first 40 days of the time series amounts to only 3.1×10^{19} N.m, about 90% of the observed postseismic deformation was aseismic. The distribution of aftershocks is correlated with the distribution of afterslip, consistent with the notion that aftershocks are driven by afterslip (e.g., Perfettini and Avouac, 2004; Hau et al., 2006).

Fault slip derived from the modeling of the geodetic time series from 20 to 408 days after the mainshock. The model shown here allows a variable rate. The weight put on smoothing and the choice of 3 principal components is justified from a Chi-square test. The 2 m slip contour lines of the 2007 earthquake are shown in cyan. The green contour shows the density of aftershocks in the first 40 days following the mainshock. Inset show the slip of the center of patches A and B deduced from the inversion of the geodetic measurements (black circles). Continuous lines show the theoretical displacements predicted from a rate-strengthening frictional sliding (Perfettini and Avouac, 2004) which assumes that friction increases linearly with the logarithm of the sliding velocity as observed in laboratory experiments (Marone et al., 1998).

References

Chlieh, M., J. P. Avouac, K. Sieh, D. H. Natafwidjaja, and J. Gelertczki (2008), Heterogeneous coupling of the Sumatran megathrust constrained by geodetic and paleogeographic measurements, *Journal of Geophysical Research*.

Darbuth, L. A., C. Gertsen, and D. Darbuth (1990), Assessment of the size of large and great historical earthquakes in Peru, *Bull. Seism. Soc. America*.

Goggin, K. C., D. Chadwell, and E. Nisranobas (2009), Measuring the onset of locking in the Peru-Chile trench with GPS and oceanic measurements, *Nature*.

Hau, V. J., M. (2006), Frictional afterslip following the 2005 Nias-Simulau earthquake, *Sumatra, Science*.

Kendrick, E. M., B. Bevis, R. S. Smalley, and B. Brooks (2001), An integrated crustal velocity field for the Central Andes, *Geochim. Geophys. Resear.*

Kasitsky, A., and J. P. Avouac (2009), Inverting geodetic time series with a Principal Component Analysis based Inversion Method, *Journal of Geophysical Research*.

Langer, C. J., and W. Spence (1995), The 1974 Peru Earthquake Series, *Bulletin of the Seismological Society of America*.

Marone, C. (1998), Laboratory-derived friction laws and their application to seismic faulting, *Annual Review of Earth and Planetary Sciences*.

Perfettini, H., and J. P. Avouac (2004), Stress transfer and strain rate variations during the seismic cycle of the subduction megathrusts, *J. Geophys. Res.*

Sladen, A. et al. (2009) Source Model of the 2007 Mw8.0 Pisco, Peru earthquake-implications for seismogenic behavior of subduction megathrusts, *J. Geophys. Res.*

Introduction

The seismic hazard on any major fault depends primarily on the partitioning between aseismic and aseismic slip. Identifying where and when aseismic creep is taking place and what fraction of long-term motion it accounts for are therefore critical questions. Slip is almost purely aseismic on megathrust at depth greater than about 40 km. At shallower depths, aseismic slip is probably generated as both modes of slip occur leading to heterogeneous strain (e.g., Chlieh et al., 2008). Aseismic slip can occur as result of steady or transient creep in the interseismic and postseismic periods. This megathrust seems to comprise areas that readily slip during earthquakes (governed by a rate-strengthening friction law), and areas that mostly slip aseismically (governed by rate-strengthening friction law).

Here we try to image the patchwork of rate-strengthening and rate-weakening areas that pave the Megathrust offshore southern Peru, using geodetic observations of postseismic deformation following the Mw8.0 Pisco earthquake of 2007. The source model of that earthquake (Sladen et al., 2009), and geodetic measurements of interseismic strain acquired before that earthquake.

Discussion

Our modeling results show that the post- and co-seismic slip distributions complement each other (the small overlap might simply reflect the smoothing effect of the regularization). This observation is consistent with the view that the shallow portion of the megathrust is paved with areas that are rate-weakening within which earthquakes can nucleate and propagate, and areas that are rate-strengthening within which slip is mostly aseismic. In that regard, we speculate that the two asperities that we identify in this study are rate-strengthening and rate-weakening patches (labeled A and B). A most striking finding is that the prominent aseismic patch (labeled A) coincides with the northern side of the Nazca ridge where the 2007 rupture stopped. Interestingly, none of the Mw > 8 horizontal earthquakes which have occurred either north (1687, 1746) or south (1604, 1868) of Pisco in the past 500 years, seem to have ruptured areas that particular patch of the megathrust (see (1)). Thus, we infer that this patch is a permanent barrier characterized by a rate-strengthening friction, possibly related to the subduction of the Nazca ridge beneath the South American plate. The rupture of the 2007 Pisco earthquake and the Nazca ridge subducts beneath the forearc: is also visible from the pattern of interseismic strain. Modeling of the interseismic geodetic data indeed shows a locally low interseismic coupling in this area (between latitudes 11°S and 16°S) where the 1974 Lima earthquakes coincide with higher coupling. The morphology of the forearc, characterized by an interruption of the forearc basin and a narrower distance from the trench to the coastline also probably reflects the effect of the Nazca ridge.

With regard to the aseismic/aseismic slip budget, the modeling of interseismic signals that 41.6±2% of the long-term interplate slip results from aseismic slip in the interseismic period (see (6)). The remaining fraction must result from transient aseismic or aseismic slip. Assuming that the ratio between the moments released by afterslip and by aseismic slip is about 30%, as typically found for large megathrust earthquakes, aseismic would contribute between 50% and 70% of the total slip. This might still be an underestimate since the possibility of spontaneous aseismic transients is ignored.

The interseismic coupling model suggests a moment deficit accumulation rate of 0.63×10^{19} N.m/yr in the area that ruptured during the Pisco earthquake (latitude 13°S to 15°S, depth lower than 40 km). At this rate, we estimate it would take 250 yr to accumulate a deficit of moment equivalent to the 1.5×10^{21} N.m moment released by aseismic and the afterslip during the Pisco earthquake. This estimate is close to the 260 years between the 2007 Pisco earthquake and the previous large megathrust earthquake in this area which occurred in 1746.